DP-1600

CURIUM-245 AND CURIUM-247 NEUTRON CROSS SECTIONS BETWEEN 10 keV AND 10 MeV

LOREN R. CLIFFORD AND
F. JOSEPH McCROSSON

E. I. du Pont de Nemours & Co.
Savannah River Laboratory
Aiken, SC 29808

PREPARED FOR THE U. S. DEPARTMENT OF ENERGY UNDER CONTRACT DE-AC09-76SR00001

Printed in the United States of America

Available from

National Technical Information Service
U S Department of Commerce
5285 Port Royal Road
Springfield, Virginia 22161

Price: Printed Copy A04; Microfiche A01

726936

DP-1600

Distribution Category UC-34c

CURIUM-245 AND CURIUM-247 NEUTRON CROSS SECTIONS BETWEEN 10 keV AND 10 MeV

Loren R. Clifford
Central Michigan University, Mount Pleasant, Michigan

and

F. Joseph McCrosson
E. I. du Pont de Nemours and Co.
Savannah River Laboratory

Approved by
P. L. Roggenkamp, Research Manager
Operational Planning Division

Publication Date: July 1982

E. I. du Pont de Nemours & Co.
Savannah River Laboratory
Aiken, SC 29808

PREPARED FOR THE U. S. DEPARTMENT OF ENERGY UNDER CONTRACT DE-AC09-76SR00001

ABSTRACT

The optical model code 2PLUS and the statistical model codes COMNUC and CASCADE were used to compute neutron cross sections for Cm-245 and Cm-247 between 10 keV and 10 MeV. Cross sections for elastic and inelastic scattering, radiative capture, fission, and the (n,2n) reactions were computed. The parameters for the fission model were selected to yield agreement with the cross sections from the Physics-8 bomb shot. Pu-239 cross sections were calculated and compared with existing cross section evaluations to demonstrate the validity of the calculational methods.

CONTENTS

INTRODUCTION

Accurate prediction of curium assays in reactor-irradiated fuels is required both for forecasting californium production and for evaluating fuel recycle strategies and their implications for waste management. The chain for producing curium and californium isotopes from Pu-242 by successive neutron captures is given in Figure 1. It is desirable to have cross sections for these nuclides which extend from very low energies up to at least 10 MeV. The capture and fission cross sections below 10 keV are of prime importance in thermal and near-thermal reactor irradiations, whereas the cross sections above 10 keV are important in fast reactors.

Savannah River Laboratory in 1975 completed a study which yielded a consistent set of cross sections below 10 keV for the nuclides in Figure 1.[1] The study utilized differential and integral cross section measurements and production data from SRP irradiations. These cross sections, originally cast in multigroup form, have been transferred to the ENDF/B pointwise energy format,[2] and with some modifications and improvements are a part of the latest Evaluated Nuclear Data File release, ENDF/B-V. These data are available for distribution from the National Nuclear Data Center (NNDC) at Brookhaven National Laboratory.

The preceding ENDF/B cross section file, ENDF/B-IV, released in 1974, contains high energy data for only three of the nuclides in Figure 1: Pu-242, Am-243, and Cm-244. SRL has performed nuclear model calculations for the high energy cross sections of Cm-246 and Cm-248.[3] The Cm-245,-247 calculations described in this report serve to complete the important cross section data for the curium isotopes. The Cm-245,-246,-247,-248 high energy evaluations have been sent to NNDC and are available in ENDF/B-V.

Since only fission cross section measurements over a limited energy range have been performed, it was necessary to determine the high energy Cm-245,-247 cross sections using nuclear models. The SRL version of the optical model code 2PLUS[4] was used to determine nuclear penetrabilities and the total, shape elastic and direct inelastic cross sections as a function of energy. 2PLUS was written for even A nuclei, but was found to be adaptable for use with odd A targets as well. The 2PLUS penetrabilities were used in the statistical model codes COMNUC and CASCADE[5] to determine

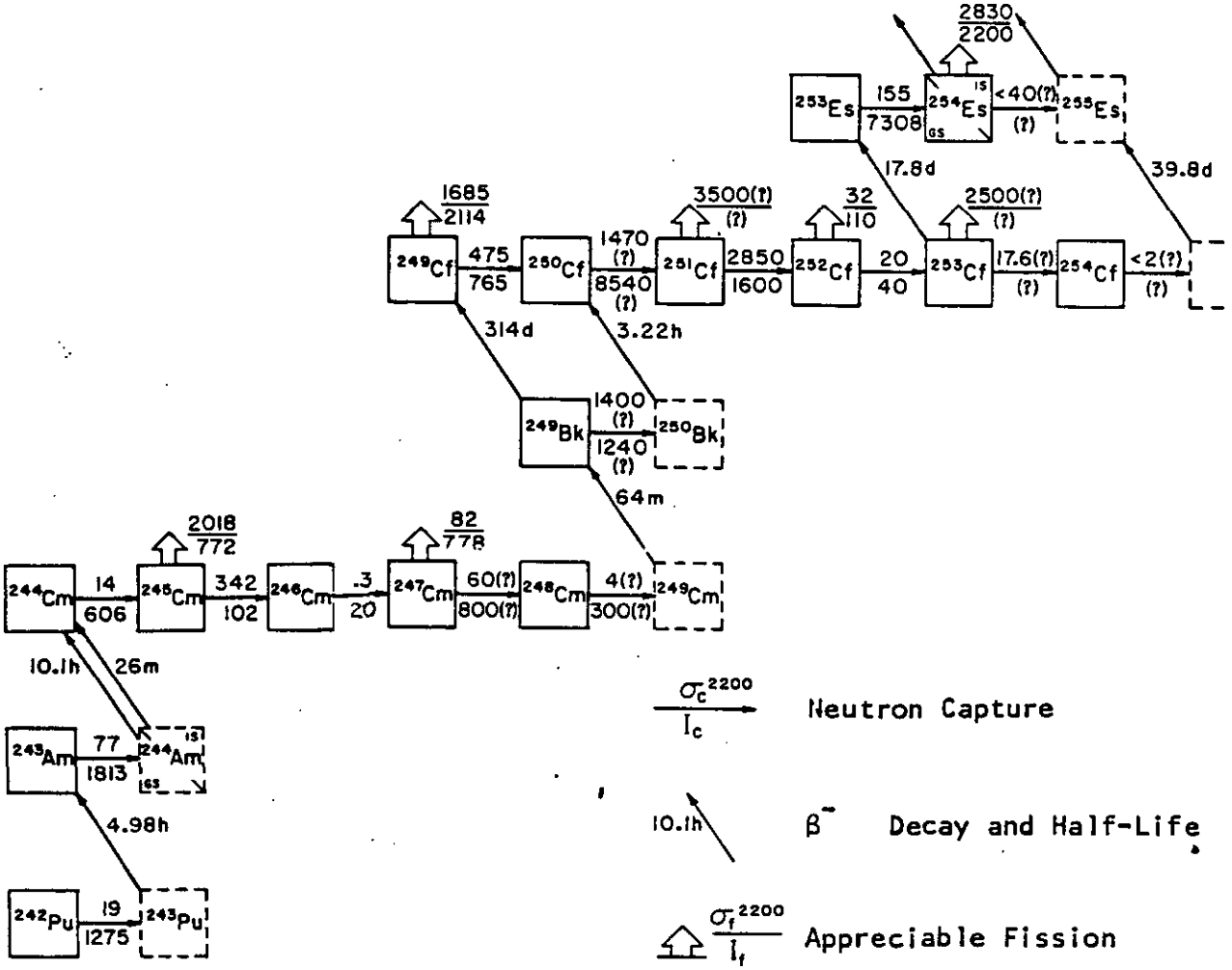

FIGURE 1. The ^{252}Cf Production Chain

the cross sections associated with compound nucleus decay: compound elastic and inelastic scattering, radiative capture, fission, and (n,2n). The CASCADE code also provided input to COMNUC to represent gamma and neutron cascade processes.

Before performing the Cm-245,-247 calculations, the techniques were tested on Pu-239. Pu-239 was selected since, of the nuclides where extensive cross section measurements have been performed, its nuclear properties are most like those of Cm-245 and Cm-247. The Pu-239 calculation served to validate the calculational techniques, particularly for direct inelastic scattering. Also, they provided a measure for estimating the accuracy of the Cm-245,-247 results.

SUMMARY

The calculated cross sections for Pu-239 agreed reasonably well with the evaluated Pu-239 cross sections of ENDF/B-III. A summary of the comparison follows:

TABLE 1

Reaction Type	Energy Range, MeV	Typical Deviation from ENDF/B-III Data
σ_T	0.01-10	0%
σ_{el}	0.01-10	5%
σ_c	0.01-0.1	15%
	0.1-1.0	50%
	1.0-2.0	30%
σ_f	0.01-2.5	5%
	2.5-6.0	20%
	6.0-10.0	5%
σ_{in}	0.01-0.1	50%
	0.1-1.0	20%
	1.0-10.0	10%

The total cross section agreed at all energies because the optical model parameters were adjusted to achieve this result. The large difference between the calculated and evaluated radiative capture cross section above 0.1 MeV is not unexpected due to the relative smallness of the cross section in this energy region. The 50% deviation between the calculated and evaluated inelastic cross section below 0.1 MeV is attributed to the simplified model for direct inelastic scattering used in this work.

Of the Cm-245 and Cm-247 cross sections, only the fission cross sections have been measured at energies in the fast region[6] (up to about 3 MeV). The nuclear model calculations of this study yielded reasonably good agreement with the measured Cm-245,-247 fission cross sections. Differences from experiment were typically 10%, although individual points were off by 25%. The methods of calculation were identical for Pu-239 and Cm-245,-247 and the input parameters for the calculations, e.g., optical model parameters,

neutron binding energies, energy level schemes, and strength functions for radiative capture, are known with about the same degree of confidence for Pu-239 and Cm-245,-247. Thus, the accuracies of the calculated Cm-245,-247 cross sections are expected to be comparable to those for Pu-239, viz. the differences from ENDF/B-III shown in the above table. The total cross sections are assumed to have 5% accuracy. The calculated Cm-245,-247 cross sections are given in Tables 8 through 13 of this report.

DISCUSSION

Theory - General Concepts

Reaction Types and Channels

Fast neutrons have energies in the range 0.5 MeV < E < 10 MeV. Neutron cross sections in this region are smooth functions of energy. The upper limit, 10 MeV, is below the threshold for charged particle emission; the lower limit, 0.5 MeV, is above the region where resonances are resolved. The present calculation was extended down to 10 keV to see the trend of the cross sections beyond the lower limit. The various cross sections which make up the total cross section, σ_T, are the elastic, inelastic, capture, fission, and (n,2n) cross sections.

$$\sigma_T = \sigma_{el} + \sigma_{in} + \sigma_c + \sigma_f + \sigma_{n,2n} \qquad (1)$$

For the purpose of calculation with the compound nucleus theory, σ_T is divided into a direct elastic cross section $\sigma_s(1)$ (also called the shape elastic cross section σ_{se}), some direct inelastic cross sections $\sigma_s(i)$ i = 2,3, ... which correspond to the levels of the target nucleus, and an absorption cross section σ_a.

$$\sigma_T = \sum_i \sigma_s(i) + \sigma_a \qquad (2)$$

The direct elastic and inelastic components $\sigma_s(i)$ correspond to scattering without the intermediate process of absorption of the neutron by the target nucleus. The absorption component σ_a is the cross section for the formation of the compound nucleus. The various scattering processes are pictured in Figure 2. The target nucleus with charge Z and mass A is assumed to be in its ground state. If the absorbed neutron has an incident energy E, the compound nucleus has charge Z, mass A+1, and excitation energy E+U, where U is the neutron separation energy (binding energy of the last neutron in the compound nucleus).

$$U = \left[M(Z,A) + M_n - M(Z,A+1)\right] c^2 \qquad (3)$$

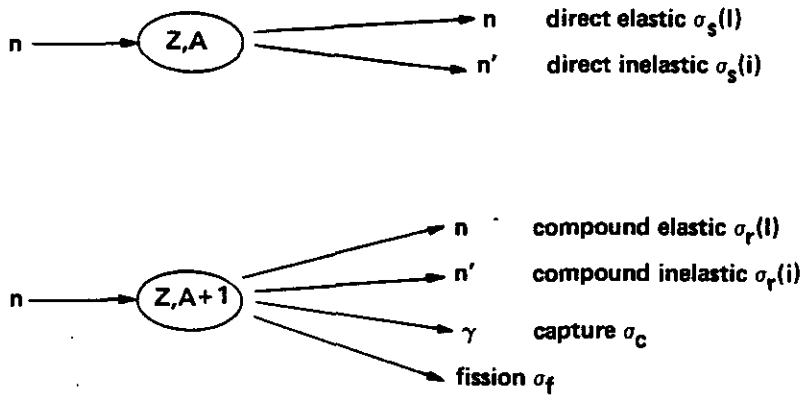

FIGURE 2. Scattering Processes

The quantities in the brackets are respectively the mass of the target, the mass of a neutron, and the mass of the compound nucleus.

The absorption cross section is the sum

$$\sigma_a = \sum_i \sigma_r(i) + \sigma_c + \sigma_f + \sigma_{n,2n} \tag{4}$$

The compound elastic cross section $\sigma_r(1)$ corresponds to emission of a neutron from the compound nucleus with the same energy E as the incident neutron energy. The elastic cross section is the sum of the direct elastic and compound elastic cross sections

$$\sigma_{el} = \sigma_s(1) + \sigma_r(1) \tag{5}$$

The compound inelastic cross sections $\sigma_r(i)$ i = 2,3, ... are also added to their direct counterparts

$$\sigma_{in}(i) = \sigma_s(i) + \sigma_r(i) \qquad i = 2,3, \ldots \tag{6}$$

and $\sigma_{in}(i)$ is the cross section for scattering of a neutron which leaves the target in an excited energy level E_i. The inelastic cross section is then

$$\sigma_{in} = \sum_i \sigma_{in}(i) \tag{7}$$

and corresponds to all neutron scattering processes where the final neutron energy is less than E. The capture cross section σ_c corresponds to the capture of the incident neutron followed by the emission of a photon from the compound nucleus. In the case of fission, some of the excitation energy is used to distort the nuclear surface. For nuclei with sufficiently large values of Z^2/A there is a critical distortion beyond which the long-range repulsive Coulomb force can dominate the short-range attractive nuclear force with the result that fission occurs.[7] The (n,2n) reaction is a neutron cascade in which one neutron is emitted and then another neutron is emitted. The second neutron emission is energetically possible only if the excitation energy of the compound nucleus (Z,A+1) is greater than U + U', where U' is the separation energy for the second neutron.

$$U' = \left[M(Z,A-1) + M_n - M(Z,A)\right] c^2 \tag{8}$$

The values of U and U' used in this report were taken from Lynn[8] and are presented in Table 2. The threshold for the (n,2n) reaction is E = U'.

TABLE 2

Separation Energies

Target	Compound Nucleus	U, MeV	U', MeV
Pu-239	Pu-240	6.52	5.66
Cm-245	Cm-246	6.45	5.52
Cm-247	Cm-248	6.21	5.16

In order to discuss the calculation of the cross sections, it is necessary to introduce the concept of channels. A channel is a state of the total system, e.g., a state of the neutron and nucleus. It is adequate in this discussion to represent a channel by the quantum numbers for energies, parities, and spins. The various channels are shown in Figure 3. The angular momentum of the relative motion ℓ is added to the neutron spin to form j. In the incident channel the neutron has incident energy E, the parity of the relative motion is $(-1)^{\ell}$ and the angular momentum j has the values $j = \ell \pm 1/2$. Also included in the incident channel is the initial state of the target nucleus which has the ground state energy $E_1 = 0$, parity π_1, and spin I_1. The neutron and target come together and form a compound system with energy E + U, parity $\pi = \pi_1(-1)^{\ell}$ and spin J with possible values

$$|I_1-j| \leq J \leq I_1+j \tag{9}$$

The compound nucleus then disintegrates into one of the final channels which is open, i.e., which conserves energy, parity, and spin. In each case the energy, parity, and spin of the residual nucleus is represented by E', π', I' in Figure 3. These numbers are restricted as follows. If a neutron is emitted in the state E-E', ℓ', j', then $0 \leq E' \leq E$, $\pi' = \pi(-1)^{\ell'}$ and $|J-j'| \leq I' \leq J+j'$. In the case of gamma emission, it is assumed that the radiation is of the electric dipole type so that $0 \leq E' \leq E+U$, $\pi' = -\pi$, and $|J-1| \leq I' \leq J+1$. The surface distortion which precedes a fission process is represented in terms of spherical harmonics in the continuum model and thus is assigned an angular momentum number ℓ'. The possible states of the residual nucleus (i.e., the distorted nucleus) are $0 \leq E' \leq E+U$, $\pi' = \pi(-1)^{\ell'}$, and $|J-\ell'| \leq I' \leq J+\ell'$. The various cross sections which make up the absorption

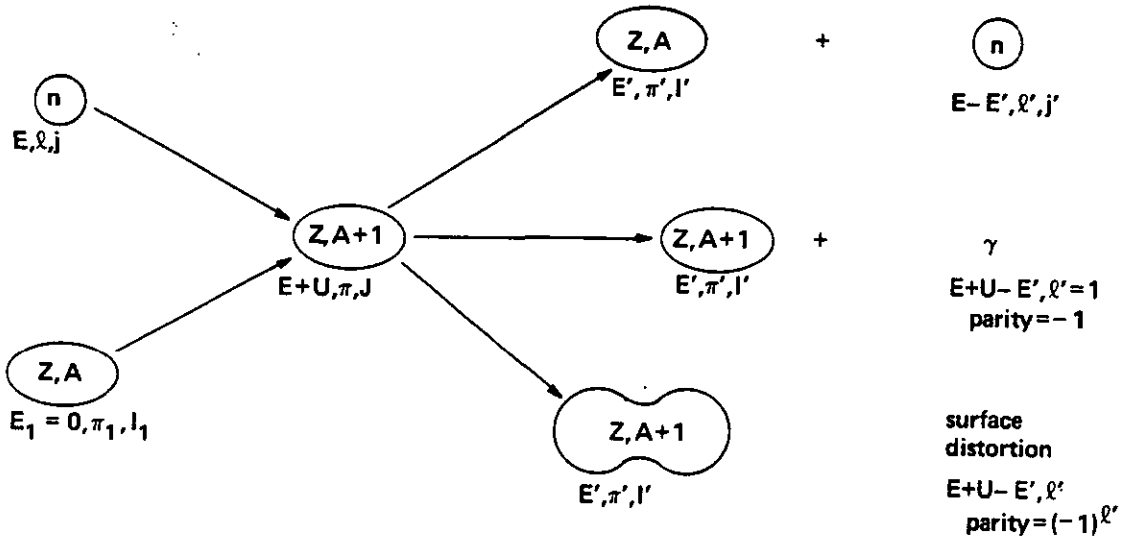

FIGURE 3. Various Channels

cross section are obtained by performing summations over all initial and final channels that are open and which correspond to a reaction of a given type. In what follows an incident channel will be denoted by c, and a final channel by c'. Thus, c stands collectively for the quantities E, ℓ, j, E_1=0, π_1, I_1. If c' is a neutron emission channel, it stands for E-E', ℓ', j', E', π', I'. If c' is a photon emission channel, it denotes E+U-E', ℓ'=1, photon parity = -1, E', π', I'. If c' is a fission channel in the continuum model it denotes E+U-E', ℓ', parity $(-1)^{\ell'}$, E', π', I'. The channels for the discrete parts of the neutron and fission models will be discussed under Statistical Models.

Cross Sections

As a first approximation it is assumed that the compound system Z,A+1,E+U,J,π "forgets" the initial channel c of its formation so that its formation in channel c and disintegration in channel c' may be regarded as independent processes linked only by conservation of energy, parity, and spin. The cross section for a process c → J, π → c' can then be written in the form

$$\sigma_{cc'} = \frac{\pi}{k^2} \frac{(2J+1)}{2(2I_1+1)} \; T_c^{J\pi} \; G_{c'}^{J\pi} \tag{10}$$

where the dependence on c and c' is contained in separate factors $T_c^{J\pi}$ and $G_{c'}^{J\pi}$. The factor $T_c^{J\pi}$ is referred to as the transmission coefficient (or penetrability) for channel c. This name derives from the old continuum theory of nuclear cross sections[9,10] in which $T_c^{J\pi}$ was literally the transmission coefficient, i.e., the probability that the incident neutron enters the nucleus. The factor $G_{c'}^{J\pi}$ is called the branching probability for the final channel c'. The branching probabilities are normalized to unity

$$\sum_{c'} G_{c'}^{J\pi} = 1 \tag{11}$$

where the sum is over all open channels c' for the given compound system J,π. The propagation number k in formula (10) is related to the incident energy E (in the C.M. coordinate system) by

$$E = \frac{\hbar^2 k^2}{2\mu} \tag{12}$$

where μ is the reduced mass of neutron and target nucleus. The statistical factor $(2J+1)/2(2I_1+1)$ takes account of magnetic quantum numbers and represents a sum over the $2J+1$ orientations of the compound nucleus spin and an average over the two orientations of the incident neutron spin and over the $2I_1+1$ orientations of the target nucleus spin.

The branching probabilities can be expressed in terms of the transmission coefficients. The time reversal symmetry of the scattering matrix implies the reciprocity

$$T_c^{J\pi} \; G_{c'}^{J\pi} = T_{c'}^{J\pi} \; G_c^{J\pi} \tag{13}$$

and this relation together with Eq. (11) gives the result

$$G_{c'}^{J\pi} = T_{c'}^{J\pi} \Big/ \sum_{c''} T_{c''}^{J\pi} \tag{14}$$

where the sum in the denominator is over all open channels. Thus, the basic problem is the calculation of the transmission coefficients for all channels. The cross section for the process $c \to J, \pi \to c'$ can now be written as

$$\sigma_{cc'}^{J\pi} = \frac{\pi}{k^2} \frac{(2J+1)}{2(2I_1+1)} \frac{T_c^{J\pi} \; T_{c'}^{J\pi}}{\sum_{c''} T_{c''}^{J\pi}} \tag{15}$$

It is important to see the relationship between the smooth cross section given by Eq. (15) and the resonance representation of the same cross section

$$\sigma_{cc'}^{J\pi} = \frac{\pi}{k^2} \frac{(2J+1)}{2(2I_1+1)} \sum_k \frac{\Gamma_{kc}^{J\pi} \; \Gamma_{kc'}^{J\pi}}{(E_k^{J\pi}-E)^2 + (\Gamma_k^{J\pi}/2)^2} \tag{16}$$

Here $E_k^{J\pi}$ $k = 1,2, \ldots$ are the resonance energies with spacing D, $\Gamma_{kc}^{J\pi}$ is the partial width of a resonance for channel c, and the total width is

$$\Gamma_k^{J\pi} = \sum_c \Gamma_{kc}^{J\pi} \tag{17}$$

where the sum is over all open channels for the compound system J,π. If $\Gamma_{kc}^{J\pi} \ll D$ an energy average of Eq. (16) gives a cross section of the same form as the compound nucleus representation Eq. (15)[11]

$$\left\langle \frac{\Gamma_{kc}^{J\pi} \quad \Gamma_{kc'}^{J\pi}}{(E_k^{J\pi} - E)^2 + (\Gamma_k^{J\pi}/2)^2} \right\rangle = \frac{2\pi}{D} \frac{\Gamma_c^{J\pi} \; \Gamma_{c'}^{J\pi}}{\Gamma^{J\pi}} \tag{18}$$

where $\Gamma_c^{J\pi}$ and $\Gamma^{J\pi}$ are averages of the partial and total width over resonance levels. The total width need not be small compared with D. Comparison of Eq. (18) with Eq. (15) gives the fundamental relation between transmission coefficients and resonance parameters

$$T_c^{J\pi} = \frac{2\pi}{D} \Gamma_c^{J\pi} \tag{19}$$

In the fast neutron region the resonances are not resolved and the smooth cross sections obtained by energy averaging should be the same as the experimentally measured cross sections.

Theory - Optical Model

The Interaction

All of the incident channels are neutron channels. Thus, the optical model determines the total cross section and the direct elastic and inelastic cross sections. In addition, the model gives the absorption cross section and the transmission coefficients for all final neutron emission channels.

In the optical model,[12] the many-body potential $V(r_1, r_2, \ldots, r_N)$ seen by the incoming neutron is replaced by a complex potential $V_R + iV_I$ which is a function of the relative distance r between neutron and nucleus and, in the case of deformed nuclei, a function of the spherical angles $\Omega = \Theta, \phi$. This replacement is made with the understanding that the cross sections derived are energy-averaged and can correspond to experimental results only when the observed cross sections are smooth functions of energy. The real part of the potential is taken to be a Saxon potential with a spin-orbit term of the Thomas type

$$V_R(r,\Omega) = - \frac{V_R}{1 + e^{(r-R)/a}} + V_S \left(\frac{\hbar^2}{m_\pi c}\right) \frac{1}{r} \frac{d}{dr} \left(\frac{1}{1 + e^{(r-R)/a}}\right) \underline{\ell} \cdot \underline{s} \tag{20}$$

where $\hbar/m_\pi c \approx 1.4$ fm is the π-meson Compton wavelength. If the neutron channel contains the angular momentum quantum numbers, j,ℓ then

$$\underline{\ell}\cdot\underline{s} = 1/2\left[j(j+1) - \ell(\ell+1) - 3/4\right] \tag{21}$$

The imaginary part of the potential is given a derivative Saxon form

$$V_I(r,\Omega) = -\,4V_I \frac{e^{(r-R)/b}}{\left[1 + e^{(r-R)/b}\right]^2} \tag{22}$$

Nuclear deformation is introduced by letting the radius R be a function of the spherical angles

$$R(\Omega) = R\left[1 + \beta \sqrt{\frac{4\pi}{5}} \sum_{m=-2}^{+2} Y_2^m(\Omega_1) Y_2^{m*}(\Omega)\right] \tag{23}$$

where Ω_1 is the direction of the nuclear symmetry axis. The deformation parameter β is given the value 0.26,[13] and the interaction is expanded to first order in this parameter

$$V \approx \left[V_R(r) + V_I(r)\right] - \beta R \sqrt{\frac{4\pi}{5}} \left(\frac{dV_R}{dr}\right) \sum_{m=-2}^{+2} Y_2^m(\Omega_1) Y_2^{m*}(\Omega) \tag{24}$$

The spin-orbit potential is omitted in the derivative dV_R/dr and the imaginary well has also been dropped from this term because both of these contributions would involve a second derivative of the Saxon potential.

The same optical model parameters were used for Pu-239 and Cm-245,-247 and are those given by Prince[14] with the exception of the constant radius $R = r_o A^{1/3}$ fm. The Prince parameters are

$$V_R = 46.53 - 0.29E \qquad \text{(E in MeV)}$$

$$V_I = \begin{cases} 4.27 + 0.756E + 24.4E^2 & E \leq 0.1 \\ 4.27 + 3.64E - 4.35E^2 & 0.1 < E \leq 0.5 \\ 4.27 + 1.89E - 0.86E^2 & 0.5 < E \leq 1.0 \\ 5.0 + 0.36E & 1.0 < E \leq 4.0 \\ 5.54 + 0.202E & 4.0 < E \leq 10.0 \end{cases}$$

$$a = 0.65 \text{ fm} \qquad b = 0.47 \text{ fm} \qquad V_S = 7.0$$

The radius r_o was allowed to decrease smoothly with energy from a value of 1.35 at 0.01 MeV[15] to 1.26 at 10 MeV and was chosen to reflect ENDF/B-III data for Pu-239.

Coupled Radial Equations

The total system Hamiltonian is

$$H = H_N + T + V \tag{25}$$

where H_N is the nuclear Hamiltonian, T is the kinetic energy of relative motion between incident neutron and target, and V is the interaction of Eq. (24). The energy levels E_i of H_N are labeled so that i = 1 is the ground state and i = 2 is the first excited state. These levels have spin and parity numbers I_i, M_i, π_i. The relative angular momentum ℓ, m_ℓ is coupled to the neutron spin to form j, m_j and this in turn is coupled to I_i, M_i, π_i to form the total system angular momentum and parity J, M, π. The resulting angular momentum eigenfunctions $\Phi^{J\pi M}_{\ell j, I_i \pi_i}$ are also eigenfunctions of H_N.

The stationary states of the total system (target plus neutron) satisfy the Schrodinger equation

$$H \Psi_E^{J\pi M} = E \Psi_E^{J\pi M} \tag{26}$$

and can be expanded in terms of angular momentum eigenfunctions

$$\Psi_E^{J\pi M} = \sum_{i=1}^{\infty} \sum_{j=|J-I_i|}^{J+I_i} (i)^{\ell} \frac{u^J_{\ell j i}(r)}{r} \Phi^{J\pi M}_{\ell j,\ I_i \pi_i} \tag{27}$$

Note that ℓ is determined by j, π_i, π in this expansion since ℓ is either j+1/2 or j-1/2 and $(-1)^{\ell} = \pi\pi_i$. The coupled differential equations for the radial functions are

$$\frac{\hbar^2}{2\mu} \left[k_i^2 + \left(\frac{d^2}{dr^2} - \frac{\ell(\ell+1)}{r^2}\right)\right] u^J_{\ell j i} =$$

$$\sum_{i'=1}^{\infty} \sum_{j'=|J-I_i'|}^{J+I_i'} (j, I_i, J, M | V | j', I_i', J, M)\ u^J_{\ell' j' i'} \tag{28}$$

The propagation numbers k_i are given by

$$\frac{\hbar^2 k_i^2}{2\mu} = E - E_i \tag{29}$$

The matrix elements which couple different radial functions are taken between the eigenfunctions $(i)^{\ell}\ \Phi^{J\pi M}_{\ell j, I_i \pi_i}$. The interaction, Eq. (24), is a sum of scalar products.[16]

$$V = \sum_{k=0}^{2} \sum_{m=-k}^{+k} T_k^m\ Y_k^{m*} = \sum_{k=0}^{2} V_k \tag{30}$$

The Wigner-Eckart theorem is used to evaluate the matrix elements.

$$(j, I_i, J, M | V_k | j', I_i', J, M) = (i)^{\ell'-\ell}\ (-1)^{j+I_i'-J}\ x$$
$$W(j' I_i' j I_i, Jk)\left[(2j+1)(2I_i+1)\right]^{1/2} (I_i \| T_k \| I_i')(j \| Y_k \| j') \tag{31}$$

The reduced matrix elements are defined according to the convention of Rose,[16] page 85, and W is a Racah coefficient. A further reduction gives

$$(j \| Y_k \| j') = (-1)^{1/2+k-\ell'-j'}\left[(2\ell+1)(2j'+1)\right]^{1/2}\ x$$
$$W(\ell' j' \ell j; \tfrac{1}{2} k)\ (\ell \| Y_k \| \ell') \tag{32}$$

and the reduced matrix elements of spherical harmonics are

$$(\ell \| Y_k \| \ell') = (\ell', 0, k, 0 | \ell', k, \ell, 0)\ \left[\frac{(2\ell'+1)(2k+1)}{4\pi(2\ell+1)}\right]^{1/2} \tag{33}$$

where $(\ell', m_{\ell'}, k, m | \ell', k, \ell, m_\ell)$ is a Clebsch-Gordan coefficient.[16]

Comparison of Eq. (24) and Eq. (30) shows that the monopole term (k = 0) is

$$V_0 = V_R + iV_I = T_0^0\ Y_0^{0*} \tag{34}$$

so that

$$(I_i \| T_0^0 \| I_i') = \sqrt{4\pi}\ V_0\ \delta_{ii'} \tag{35}$$

The radial equations can therefore be put into the form

$$\left\{\frac{\hbar^2}{2\mu}\left[k_i^2 + \left(\frac{d^2}{dr^2} - \frac{\ell(\ell+1)}{r^2}\right)\right] + V_0\right\} u^J_{\ell j i} =$$

$$\sum_{i'=1}^{2} \sum_{j'=|J-I_i'|}^{J+I_i'} \left(j, I_i, J, M | V_2 | j', I_i', J, M\right) u^J_{\ell' j' i'} \tag{36}$$

where the left side contains the terms which occur for a spherical nucleus and the right side represents the coupling that results from a deformed nuclear surface. The summation over i' on the right side of Eq. (36) has been truncated to two terms, and the resulting coupled equations are used only for i = 1, 2. Thus, the ground state is coupled only to the first excited state. This approximation is intended for use only with nuclei of even mass and $I_1 = 0$, $I_2 = 2$.

The matrix element of V_2 vanishes when $I_i = I_i' = 0$ because of the identity

$$W(j'0j0;J2) = 0 \tag{37}$$

Comparison of Eq. (24) and Eq. (30) shows that

$$T_2^m = -\beta R \sqrt{\frac{4\pi}{5}} \left(\frac{dV}{dR}\right) Y_2^m(\Omega_1) \tag{38}$$

so that

$$\left(I_i \| T_2 \| I_i'\right) = -\beta R \sqrt{\frac{4\pi}{5}} \left(\frac{dV_R}{dr}\right) \left(I_i \| Y_2 \| I_i'\right) \tag{39}$$

According to Eq. (33) the required reduced matrix element is

$$\left(I_i \| Y_2 \| I_i'\right) = \left(I_i', 0, 2, 0 | I_i', 2, I_i, 0\right) \left[\frac{(2I_i'+1)(5)}{4\pi(2I_i+1)}\right]^{1/2} \tag{40}$$

Equations (31), (32), (33), (39), and (40) completely evaluate the matrix elements which appear in the coupled radial Eq. (36). The relevant Clebsch-Gordan coefficients are

$$(2,0,2,0|2,2,0,0) = 1/\sqrt{5} \tag{41a}$$

$$(0,0,2,0|0,2,2,0) = 1 \tag{41b}$$

$$(2,0,2,0|2,2,2,0) = -\sqrt{2/7} \tag{41c}$$

Scattering Matrix

In the procedure of Blatt and Biedenharn,[17] an incident wave solution is defined which corresponds to neutrons traveling parallel to the z-axis with spin m_s.

$$\Psi_E^{J\pi(M_1+m_s)}(\text{inc}) = \sum_{j=|I_1-j|}^{I_1+j} (i)^{\ell} A_{\ell j}^{J\pi} \frac{1}{r} [u_{\ell}^{-}(k_1 r) - u_{\ell}^{+}(k_1 r)] \times \Phi_{\ell j, I_1 \pi_1}^{J\pi(M_1+m_s)} \tag{42}$$

Here we introduce the propagation number $k_1 = k$ which corresponds to the ground state $E_1 = 0$ of the target nucleus. When $I_1 = M_1 = 0$,

$$A_{\ell j}^{J\pi} = \frac{i}{k_1} \pi^{1/2} \sqrt{2\ell+1} \quad (\ell,1/2,J,m_s|\ell,0,1/2,m_s) \; \delta_{jJ} \tag{43}$$

In the presence of scattering the outgoing wave takes on contributions from channels other than the incident ones and the solution becomes

$$\Psi_E^{J\pi(M_1+m_s)}(\text{scat}) = \sum_{i=1}^{2} \sum_{j=|J-I_i|}^{J+I_i} \left(\frac{k_1}{k_i}\right)^{1/2} (i)^{\ell} \times \left[A_{\ell j}^{J\pi} \; \delta_{i1} \frac{u_{\ell}^{-}(k_i r)}{r} - B_{\ell j;i}^{J\pi} \frac{u_{\ell}^{+}(k_i r)}{r}\right] \Phi_{\ell j, I_i \pi_i}^{J\pi(M_1+m_s)} \tag{44}$$

The new coefficients are related to the old ones by the scattering matrix elements

$$B^{J\pi}_{\ell j;i} = \sum_{\ell' j' i'} S^{J\pi}_{\ell j i;\ell' j' i'} A^{J\pi}_{\ell' j'} \delta_{i'1} \tag{45}$$

The direct elastic cross section and the direct inelastic cross section for the first excited state (assumed to be a 2^+ state in the 2PLUS model) take the form with i' = 1, 2

$$\frac{d\sigma_s(i')}{d\Omega} = \frac{1}{k^2} \frac{1}{2(2I_1+1)} \sum_{L=0}^{\infty} B_L(i') P_L(\cos\theta) \tag{46}$$

where the coefficients $B_L(i')$ depend upon the S-matrix elements. The evaluation of these coefficients is discussed by Blatt and Biedenharn. In the present work only the cross sections integrated over angles were computed and these involve $B_0(i')$. The result is

$$\sigma_s(i') = \frac{\pi}{k^2} \frac{1}{2(2I_1+1)} \sum_{J,\pi} (2J+1) \times \tag{47}$$

$$\sum_{j=|J-I_1|}^{J+I_1} \sum_{j'=|J-I_i'|}^{J+I_i'} \left| \delta_{\ell'\ell} \delta_{j'j} \delta_{i'1} - S^{J\pi}_{\ell' j' i';\ell j 1} \right|^2$$

For i' = 1 this is the direct elastic cross section referred to in Eq. (2). For i' = 2, Eq. (47) is the direct inelastic cross section for excitation of the first excited state. Direct inelastic cross sections for higher excited states are not computed by the 2PLUS code.

The absorption cross section, which is a result of the imaginary part of the interaction, is

$$\sigma_a = \frac{\pi}{k^2} \frac{1}{2(2I_1+1)} \sum_{J,\pi} (2J+1) \sum_{j=|J-I_1|}^{J+I_1} T^{J\pi}_{\ell j 1} \tag{48}$$

where the penetrabilities are

$$T^{J\pi}_{\ell j i} = 1 - \sum_{\ell' j' i'} \left| S^{J\pi}_{\ell' j' i';\ell j i} \right|^2 \tag{49}$$

and the indices i and i' take the values 1, 2. The absorption cross section is viewed as the cross section for formation of the compound nucleus in the initial channels c and disintegration into final channels c'.

$$\sigma_a = \frac{\pi}{k^2} \frac{1}{2(2I_1+1)} \sum_{J,\pi} \sum_{c,c'} (2J+1) \; T_c^{J\pi} \; G_{c'}^{J\pi} \tag{50}$$

The initial channel transmission coefficients are

$$T_c^{J\pi} = T_{\ell j 1}^{J\pi} \tag{51}$$

The transmission coefficients for final channels that correspond to compound elastic scattering are also given by Eq. (51). For compound inelastic scattering that leaves the nucleus in its first excited state, the final channel transmission coefficients are

$$T_{c'}^{J\pi} = T_{\ell j 2}^{J\pi} \tag{52}$$

Since the 2PLUS theory couples only the first two levels, compound inelastic scattering that leaves the nucleus in levels higher than the first excited state can be represented by transmission coefficients calculated from a spherical optical model. Let these be denoted by

$$T_{c'}^{J\pi} = T_{\ell j i}^{J\pi} \qquad i = 3, 4, \ldots \tag{53}$$

Instead of introducing a spherical optical model, the present calculation used the elastic penetrabilities.

$$T_{\ell j i}^{J\pi} = T_{\ell j 1}^{J\pi} \left(E-E_i\right) \qquad i = 3, 4, \ldots \tag{54}$$

The energy argument is shifted to represent the energy of the emitted neutron.

The total cross section obtained from the optical model is

$$\sigma_T = \frac{\pi}{k^2} \frac{1}{2(2I_1+1)} \sum_{J,\pi} (2J+1) \; x \tag{55}$$

$$\sum_{j=|J-I_1|}^{J+I_1} \left[2 - S_{\ell j 1;\ell j 1}^{J\pi} - S_{\ell j 1;\ell j 1}^{J\pi *}\right]$$

This satisfies the equation

$$\sigma_T = \sigma_a + \sigma_s(1) + \sigma_s(2) \qquad (56)$$

If the sum over i' in Eq. (36) had not been truncated, Eq. (2) would represent the more general result where the sum includes all levels E_i that can be excited by the incident energy. An attempt was made to compensate for the discrepancy between Eq. (2) and Eq. (56) by adding another direct inelastic cross section to both σ_{in} and σ_T at incident energies above 2.5 MeV. The nuclear radius r_o was chosen to fit the total cross section of Pu-239 for $E < 2.5$ MeV. For the region above 2.5 MeV, r_o was chosen to fit the elastic cross section, and the total cross section (and direct inelastic cross section) was supplemented by the amounts shown in Table 3.

TABLE 3

Adjustments to the Direct Inelastic Cross Section

Energy, MeV	$\Delta\sigma_T$ (= $\Delta\sigma_{in}$), barns
2.5	0.17
3.0	0.34
4.0	0.43
5.0	0.36
6.0	0.26
7.0	0.25
8.0	0.29
9.0	0.25
10.0	0.25

2PLUS With Odd A Target

The 2PLUS code assumes that $I_1 = 0, \pi_1 = +1$ and $I_2 = 2, \pi_2 = +1$. In the present work 2PLUS was applied to nuclei with odd mass and half integral spin. This is accomplished by viewing the nucleus as a single nucleon coupled to an even A core. If the core is spherical, the angular momentum j_n of the single nucleon is conserved and combines with the angular momentum I_c of the even A core to form total nuclear angular momenta I_i in the range $|I_c - j_n| \leq I_i \leq I_c + j_n$. The resulting level splitting is called a "core multiplet" by de-Shalit.[18] In this model the total nucleus

ground state consists of a core ground state with $I_c = 0$ plus a single particle with angular momentum ℓ_n, j_n. The total nucleus ground state has spin $I_1 = j_n$ and parity $\pi_1 = (-1)^{\ell_n}$. An excited core multiplet can exist with $I_c = 2$ (first excited state of the core) and with the single particle state unchanged. This multiplet would have total nuclear angular momenta $|2-j_n| \leq I_i \leq 2+j_n$ and parity the same as the ground state parity. The single particle-core excitation model was used to describe inelastic proton scattering from Ag-107.[19] The direct inelastic cross section for excitation of the excited state multiplet member with spin I_i is

$$\sigma_s(i) = \frac{(2I_i+1)}{(2j_n+1)(2I_c+1)} \sigma_s(2^+) \tag{57}$$

where $I_c = 2$ and $\sigma_s(2^+)$ is the direct inelastic cross section for the 2^+ first excited state of the even A core as computed by 2PLUS. The weight factor is the number of orientations of I_i divided by the number of combined orientations of j_n and I_c. Note that

$$(2j_n+1)(2I_c+1) = \sum_{I_i=|I_c-j_n|}^{I_c+j_n} (2I_i+1) \tag{58}$$

so that $\sigma_s(2^+)$ is divided among the members of the multiplet by Eq. (57).

In the case of deformed nuclei, the low lying spectrum consists of rotation bands. Each band is based on a particular intrinsic single particle configuration. The motion of a single nucleon in the potential field of a deformed core was described by Nilsson.[20] The nucleon angular momentum is not constant in the field of the deformed core; however, $(j_n)_z$ and $(\ell_n)_z$ are constants of the motion (z-axis along the nuclear symmetry axis). A rotation band begins with $I_i = (j_n)_z$ and successive levels of the band have spins I_i which increase in steps of unity.

When $(j_n)_z = 1/2$ in the rotor model of deformed nuclei, and $j_n = 1/2$ in the vibrator (core excitation) model of non-deformed nuclei, there is a correspondence between the spin assignments of the first three levels:

rotor model with $(j_n)_z = 1/2$	$I_i = 1/2, 3/2, 5/2$	
core excitation model with $j_n = 1/2$	$I_c = 0$	$I_i = 1/2$
	$I_c = 2$	$I_i = 3/2, 5/2$

This coincidence has been used to apply Eq. (57) to neutron scattering from W-183 which is a deformed nucleus with a low lying spectrum consisting of rotational bands.[21] The use of this procedure when $I_1 = 1/2$ is corroborated by the calculation of Prince[14] who used the coupled channel code, Jupiter I. The direct inelastic cross sections for the $3/2^+$ and $5/2^+$ states of Pu-239 are roughly in the ratio of 2:3 as predicted by Eq. (57).

In the present work a fictitious 2^+ level at 0.04 MeV was assumed for the 2PLUS calculation. For Pu-239 the computed direct inelastic cross section $\sigma_s(2^+)$ was divided between the first two excited states (0.00785 MeV and 0.05727 MeV) in accordance with Eq. (57). Since the ground states of Cm-245,-247 are $7/2^+$ and $9/2^-$ and their first excited states lie relatively high at 0.055 MeV and 0.061 MeV, $\sigma_s(2^+)$ was simply assigned to the first excited state in the case of these two isotopes.

The other accommodation of the 2PLUS code to the present odd A target calculations was the manner in which penetrabilities were assigned to energy levels. The COMNUC code accepts neutron penetrabilities in an ℓ,j format. Since 2PLUS assumes $I_1 = 0$, $\pi_1 = +1$, the elastic penetrabilities $T_{\ell j1}^{J\pi}$ already depend only on ℓ,j since $J = j$ and $\pi = (-1)^\ell$. The 2^+ level penetrabilities $T_{\ell j2}^{J\pi}$ must be averaged over J values to make them suitable for input to COMNUC. The transmission coefficients used for the first two excited states of Pu-239 and for the first excited states of Cm-245,-247 are given by

$$T_{\ell j}(2^+) = \sum_J (2J+1)\, T_{\ell j2}^{J\pi} \Big/ \sum_J (2J+1) \qquad (59)$$

where the sum runs over the values $|2-j| \leq J \leq 2+j$ and $\pi = (-1)^\ell$. For higher excited states the elastic penetrabilities were used in accordance with Eq. (54).

Theory - Statistical Models

Neutron Emission

The compound elastic and inelastic cross sections involve emission of a neutron from the compound nucleus. The spectrum of the residual nucleus is represented by a few discrete low-lying levels plus a continuous level density above these. The discrete levels used in this study are given in Table 4 and were taken either from the Table of Isotopes[22] or from Nuclear Data Sheets (Academic Press). The level density formula $\rho(I',\pi',E')$ is supplied by the COMNUC and CASCADE codes and is discussed in Reference 23.

TABLE 4

Discrete Levels of the Target Nuclei

Level	Pu-239		Cm-245		Cm-247	
	$\pi_i x I_i$	E_i, MeV	$\pi_i x I_i$	E_i, MeV	$\pi_i x I_i$	E_i, MeV
1	+ 1/2	0.0	+ 7/2	0.0	- 9/2	0.0
2	+ 3/2	0.00785	+ 9/2	0.0550	- 11/2	0.061
3	+ 5/2	0.05727	+ 11/2	0.1220	- 13/2	0.137
4	+ 7/2	0.07571	+ 13/2	0.205	+ 5/2	0.225
5	+ 9/2	0.16375	+ 5/2	0.2527	+ 7/2	0.264
6	+ 11/2	0.193	+ 7/2	0.2957	+ 9/2	0.315
7	+ 5/2	0.2855	+ 3/2	0.35	+ 1/2	0.406
8	+ 7/2	0.3301	+ 9/2	0.3587	+ 3/2	0.434
9	+ 9/2	0.388	- 9/2	0.3884	+ 5/2	0.450
10	- 7/2	0.3916	+ 11/2	0.4200	+ 7/2	0.516
11	- 9/2	0.434	- 11/2	0.4431		
12	+ 11/2	0.461	- 13/2	0.507		
13	- 1/2	0.4698	- 15/2	0.580		
14	- 11/2	0.486	+ 1/2	0.73		
15	- 3/2	0.4922				
16	- 5/2	0.5053				
17	+ 5/2	0.5119				
18	- 7/2	0.5562				
19	+ 3/2	0.73				
20	+ 5/2	0.76				

The sum of neutron transmission coefficients over all open final channels is separated into terms that correspond to processes that leave the nucleus in one of the discrete levels E_i

$$\Theta_i^{J\pi} = \sum_{\ell,j} T_{\ell j}(E-E_i) \tag{60}$$

plus a term that corresponds to excitation of the continuum of states

$$\Theta_n^{J\pi}(\text{cont.}) = \sum_{\ell,j} \sum_{I'=|J-j|}^{J+j} \int_{E_{cut}}^{E} T_{\ell j}(E-E')\ \rho(I',\pi',E')\ dE' \tag{61}$$

Here E_{cut} is the highest discrete level used. In Eq. (60), j takes values from $|I_i-J|$ to I_i+J and ℓ is restricted to either even or odd values according to the requirement $\pi_i(-1)^{\ell} = \pi$. In Eq. (61), j takes the values 1/2, 3/2, 5/2, ... and parity conservation requires $\pi'(-1)^{\ell} = \pi$. However, since $\rho(I'\pi',E')$ is independent of π', both even and odd values of $\ell = j \pm 1/2$ appear in the sum of Eq. (61) (ρ contains a factor of 1/2 to account for the two parities $\pi' = \pm 1$). In the case of Curium-245,-247 the $T_{\ell j}$ are given by the elastic penetrability $T_{\ell j 1}^{J\pi}$ except for i = 2 which is represented by $T_{\ell j}(2^+)$ as defined by Eq. (59). The same procedure is used for Pu-239 except that $T_{\ell j}(2^+)$ is used for i = 2, 3.

The unnormalized neutron emission probability is the sum

$$\Theta_n^{J\pi} = \sum_i \Theta_i^{J\pi} + \Theta_n^{J\pi}(\text{cont.}) \tag{62}$$

The quantity $\Theta_i^{J\pi}$ is used to calculate the compound cross section for excitation of the level E_i; in particular, $\Theta_1^{J\pi}$ is used to compute the compound elastic cross section. The integrand of Eq. (61) corresponds to the emission of a neutron with energy E-E' which leaves the residual nucleus in a continuum state with spin I', parity π', and excitation energy E'.

Gamma Emission

The most important electromagnetic radiation from the compound nucleus is the electric dipole component which has angular momentum $\ell' = 1$ and parity -1. The transmission coefficient for emission of a photon of this type with energy E is approximately given by[10]

$$T_{c'}^{J\pi} \approx K\ E^3 \tag{63}$$

where K is a constant which is determined by experimental data with the help of Eq. (19). In order to compute the capture cross section, this transmission coefficient must be summed over all open gamma emission channels to form the quantity

$$\Theta_{\gamma}^{J\pi} = \sum_{c'} T_{c'}^{J\pi} \tag{64}$$

where the c' are open γ-emission channels for the compound system J,π. This summation is performed within the COMNUC code as the integral

$$\Theta_{\gamma}^{J\pi} = \sum_{I'=|J-1|}^{J+1} \int_{0}^{E+U} K\,(E+U-E')^3\,\rho(I',\pi',E')\,dE' \tag{65}$$

where $\rho(I',\pi',E')$ represents the level density of the compound nucleus with charge Z and mass A+1. Parity conservation implies $\pi' = -\pi$; however, the level density formula provided by the code is independent of the parity, i.e., both parities are assumed to be equally numerous in any range dE'. The quantity $\Theta_{\gamma}^{J\pi}$ is called the (unnormalized) gamma emission probability. The integrand of Eq. (65) corresponds to the emission of a photon with energy E+U-E', leaving the residual (compound) nucleus with energy E', parity π', and spin I'.

The connection with low energy resonance data, Eq. (19), is used to estimate the constant K. At small energies (E ≈ 0) it can be assumed that only $\ell = 0$ neutrons are absorbed so that the compound system has spins $J = I_1 \pm 1/2$. In the case of even A target nuclei with $I_1 = 0$ the only possibility would be $J = I_1 + 1/2$. From low energy resolved resonance data, the quantity $2\pi\Gamma_{\gamma}/D$ is determined. This is related to the gamma emission probabilities by the equation

$$\left[\Theta_{\gamma}^{I_1+1/2,\pi} + \Theta^{I_1-1/2,\pi}\right]_{E\approx 0} = \frac{2\pi}{D}\,\Gamma_{\gamma} \tag{66}$$

(the second term on the left is omitted if $I_1 = 0$). The constant K in the terms on the left can thus be found when the resonance data is known. The values of Γ_{γ} and D used in the present work are shown in Table 5. The value of D for Pu-239 was suggested by Prince's calculation.[14] For the curium isotopes, level spacings were determined from level density formulas,[24] with pairing and shell corrections[25] extended to heavier masses using level spacing information from the Physics-8 bomb shot.[6] The radiation widths Γ_{γ} were determined using the formula of Reference 26, but with the coefficients modified to better fit experimental data for heavy nuclides.

TABLE 5

Radiative Capture Model Parameters

Target	Compound Nucleus	Γ_γ, meV	D, eV
Pu-239	Pu-240	42.8	9.00
Cm-245	Cm-246	28.3	4.64
Cm-247	Cm-248	30.4	4.10

Fission

In the fission model of Bohr, Wheeler, and Hill, the nucleus is treated semiclassically as a uniformly charged, incompressible liquid drop with a surface tension estimated from the semi-empirical mass formula of Bethe. Distortions of the nuclear surface are expanded in terms of spherical harmonics and the distortion energy -- the change in electrostatic plus surface energies -- is expressed as a function of the expansion coefficients. In the continuum part of the fission model, a given harmonic number ℓ is assigned a critical distortion energy E_{B_ℓ} (also called the fission barrier energy). The present calculation used only $\ell = 2$ in the continuum fission model. Fission is initiated when the distortion energy is in a neighborhood of E_{B_2} of width $\hbar\omega_2$. The transmission coefficient for fission is assumed to have the Hill-Wheeler form[27]

$$T_{c'}^{J\pi} = \frac{1}{1 + \exp\left[2\pi(E_{B_2}-E)/\hbar\omega_2\right]} \tag{67}$$

where E is the distortion energy. The continuum contribution to the unnormalized fission probability is

$$\Theta_f^{J\pi}(\text{cont.}) = \sum_{I'=|J-2|}^{J+2} \int_{E_c}^{E+U} \frac{\rho(I',\pi',E')\,dE'}{1 + \exp\left[2\pi(E_{B_2}-E-U+E')/\hbar\omega_2\right]} \tag{68}$$

This continuum probability determines σ_f in the range of incident energies between 1 MeV and the threshold energy E = U' for the (n,nf) cascade reaction. The cutoff energy E_c is chosen to give the best possible fit for σ_f below 1 MeV. In Eq. (68), $\rho(I',\pi',E')$ is the level density for the compound nucleus with charge Z and mass A+1. The continuum fission model parameters are shown in Table 6.

TABLE 6

Fission Model Parameters
(Energy in MeV)

Target	Compound Nucleus	E_B	E_c	E_{B_2}	$\hbar\omega_2$
Pu-239	Pu-240	5.62	0.73	6.10	0.50
Cm-245	Cm-246	5.90	1.60	5.30	0.50
Cm-247	Cm-248	5.70	2.35	4.49	0.50

The discrete contribution to the fission probability is

$$\Theta_f^{J\pi}(\text{discrete}) = \sum_n \frac{1}{1 + \exp\left[2\pi(E_B - E - U + E_n)/\hbar\omega_n\right]} \tag{69}$$

where E_B is a fission barrier energy and the E_n are transition state energies which correspond to states of internal excitation which accompany the elongation toward fission.[28] The total unnormalized fission probability is the sum of continuum and discrete parts

$$\Theta_f^{J\pi} = \Theta_f^{J\pi}(\text{cont.}) + \Theta_f^{J\pi}(\text{discrete}) \tag{70}$$

The transition energies E_n represent a variety of collective vibrations and have been listed by Lynn[28,29] and Kikuchi.[30] The barrier energy E_B is given in Table 6. The oscillator characteristic energy $\hbar\omega_n$ was always taken equal to 0.50 MeV. Whereas E_{B2} was chosen to fit the fission peak around 2 MeV, E_B was chosen to give the best representation of σ_f at the lower energies around 10 keV. The choice of E_B together with E_c (continuum cutoff) also determined the dip in σ_f which occurs between 10 keV and 1 MeV.

In the sum, Eq. (69), only those E_n contribute which correspond to the value of J,π. A total of fifty-seven transition states were chosen on the basis of Tables 8.1 and 8.9 in Reference 28. This large number of transition states was used in order to give a uniform treatment of Pu-239 and the curium isotopes, although fewer transition states would have been adequate for Pu-239 as shown by Prince.[31] In the case of Cm-245, a low energy incident neutron with $j = 1/2$ combines with the target nucleus to form a compound system with $J^\pi = 3^+, 4^+$. Cm-247

similarly combines to form $J^{\pi} = 4^-, 5^-$. For this reason the representation of the low energy (E ≈ 10 keV) fission cross sections for these nuclides requires transition states with relatively large spins. Table 7 gives the transition states used together with their Jπ values. The vibration types are designated in terms of letters which are explained further in References 28, 29, and 30. It should be pointed out that no effort was made to vary the values of the E_n during the process of fitting σ_f.

TABLE 7

Transition States

E_n	J^{π}	Vibration Type
0.0	$0^+, 2^+, 4^+, \ldots, 8^+$	GS
0.6	$1^-, 3^-, 5^-, \ldots, 7^-$	MA
0.6	$2^+, 3^+, 4^+, \ldots, 8^+$	G
1.0	$1^-, 2^-, 3^-, \ldots, 8^-$	B
1.5	$2^-, 3^-, 4^-, \ldots, 8^-$	MA+G
1.5	$1^+, 2^+, 3^+, \ldots, 8^+$	MA+B
1.8	$0^+, 2^+, 4^+, \ldots, 8^+$	2G
1.8	$1^-, 2^-, 3^-, \ldots, 8^-$	B+G
2.1	$0^+, 2^+, 4^+, \ldots, 8^+$	N4

Cascades

The code CASCADE generates input for COMNUC to take account of two gamma cascade processes (n,γn), (n,γf) and two neutron cascade processes (n,2n), (n,nf). This is done as follows. Define the normalized branching probabilities $G_{\alpha}^{J\pi}$ $\alpha = \gamma, n, f$:

$$G_{\gamma}^{J\pi} = \Theta_{\gamma}^{J\pi} / \Theta^{J\pi} \qquad G_{n}^{J\pi} = \Theta_{n}^{J\pi} / \Theta^{J\pi} \qquad G_{f}^{J\pi} = \Theta_{f}^{J\pi} / \Theta^{J\pi} \tag{71}$$

where

$$\Theta^{J\pi} = \Theta_{\gamma}^{J\pi} + \Theta_{n}^{J\pi} + \Theta_{f}^{J\pi} \tag{72}$$

CASCADE calculates the unnormalized probability for gamma emission followed by neutron emission

$$\Theta_{\gamma n}^{J\pi} = \sum_{I'=|J-1|}^{J+1} \int_{U}^{E+U} K\,(E+U-E')^3\,\rho(I',\pi',E')\,G_n^{I'\pi'}(E'-U)\,dE' \qquad (73)$$

where $\rho(I',\pi',E')$ is the level density of the compound nucleus with charge Z and mass A+1, and U is defined by Eq. (3). Parity conservation implies $\pi' = -\pi$. Note that a neutron can be emitted only if the excitation energy after gamma emission is no less than U. The integrand of Eq. (73) has the interpretation: a gamma is emitted with energy E+U-E' leaving the compound nucleus with excitation energy E'; a neutron is emitted with energy E'-U leaving the residual nucleus in its ground state. The corresponding unnormalized probability for gamma emission followed by fission is

$$\Theta_{\gamma f}^{J\pi} = \sum_{I'=|J-1|}^{J+1} \int_{U}^{E+U} K\,(E+U-E')^3\,\rho(I',\pi',E')\,G_f^{I'\pi'}(E'-U)\,dE' \qquad (74)$$

In the code COMNUC, the emission probabilities are redefined by the equations

$$\Theta_{\gamma}^{J\pi} = \Theta_{\gamma}^{J\pi} - \Theta_{\gamma n}^{J\pi} - \Theta_{\gamma f}^{J\pi}$$

$$\Theta_{n}^{J\pi}(\text{cont.}) = \Theta_{n}^{J\pi}(\text{cont.}) + \Theta_{\gamma n}^{J\pi} \qquad (75)$$

$$\Theta_{f}^{J\pi} = \Theta_{f}^{J\pi} + \Theta_{\gamma f}^{J\pi}$$

There is no threshold energy for the gamma cascade processes, and therefore they affect the cross sections even at small energies.

The threshold for the neutron cascade processes is E = U'. The unnormalized probability for the (n,2n) process is

$$\Theta_{n,2n}^{J\pi} = \sum_{\ell,j} \sum_{I'=|J-j|}^{J+j} \int_{U'}^{E} T_{\ell j}(E-E')\,\rho(I',\pi',E')\,G_n^{I'\pi'}(E'-U')\,dE' \qquad (76)$$

where $\rho(I',\pi',E')$ is the level density of the Z,A nucleus and U' is defined by Eq. (8). Also $G_n^{I'\pi'}$ is the neutron emission probability for a compound nucleus with charge Z and mass A (corresponding to target with charge Z and mass A-1); hence, its calculation in the code CASCADE uses the transmission coefficients for a target with charge Z and mass A-1. The integrand of Eq.(76) has the interpretation: a neutron is emitted from the Z,A+1 nucleus with energy E-E' leaving the residual Z,A nucleus with excitation energy E'; a second neutron is emitted from the Z,A nucleus with energy E'-U' leaving the residual nucleus, Z,A-1 in its ground state. The second neutron emission is possible only if the excitation energy E' is no less than the separation energy U'. The corresponding unnormalized probability for the (n,nf) process is

$$\Theta_{n,nf}^{J\pi} = \sum_{\ell,j} \sum_{I'=|J-j|}^{J+j} \int_{U'}^{E} T_{\ell j}(E-E')\, \rho(I',\pi',E')\, G_f^{I'\pi'}(E'-U')\, dE' \qquad (77)$$

where $G_f^{I'\pi'}$ is the fission branching probability computed in the CASCADE code for a compound nucleus with charge Z and mass A (corresponding to a target with charge Z and mass A-1). In the code COMNUC the emission probabilities are again redefined

$$\Theta_n^{J\pi}(\text{cont.}) = \Theta_n^{J\pi}(\text{cont.}) - \Theta_{n,2n}^{J\pi} - \Theta_{n,nf}^{J\pi}$$

$$\Theta_f^{J\pi} = \Theta_f^{J\pi} + \Theta_{n,nf}^{J\pi} \qquad (78)$$

A rough calculation of cross sections for the Z, A-1 targets Pu-238, Cm-244, and Cm-246 is required for the neutron cascade effects. The n,2n and n,nf reactions for Pu-239 were satisfactorily represented by using only continuum neutron emission and fission models in CASCADE, and this procedure was followed for Cm-245,-247 as well. Whereas the gamma cascade processes affect the cross sections only slightly, the neutron cascade processes make large contributions above the threshold E = U'.

Final Cross Section Expressions

The total, shape elastic, and direct inelastic cross sections σ_T, $\sigma_{se} = \sigma_s(1)$ and $\sigma_s(i)$ are calculated by the code 2PLUS and input to the code COMNUC. The remaining cross sections are parts of the absorption cross section and are computed by COMNUC in the form

$$\sigma_\alpha(E) = \frac{\pi}{k^2} \frac{1}{2(2I_1+1)} \sum_{J,\pi} (2J+1) \sum_{\ell,j} T_{\ell j}(E)\, G_\alpha^{J\pi}(E) \tag{79}$$

where the ℓ,j summation for a given J,π is restricted by the conditions

$$(-1)^\ell \pi_1 = \pi \qquad |I_1 - J| \leq j \leq I_1 + J \tag{80}$$

Here I_1,π_1 are the target ground state spin and parity.

The compound elastic cross section $\sigma_{ce} = \sigma_r(1)$ is given by Eq. (79) with the branching probability

$$G_{ce}^{J\pi} = \Theta_1^{J\pi} \Big/ \Theta^{J\pi} \tag{81}$$

and the elastic cross section σ_{el} is then the sum in Eq. (5). The compound cross section $\sigma_r(i)$ for excitation of the level E_i of the target nucleus is given by Eq. (79) with

$$G_i^{J\pi} = \Theta_i^{J\pi} \Big/ \Theta^{J\pi} \tag{82}$$

The compound inelastic cross section σ_{in}(comp.) is obtained from Eq. (79) with

$$G_{in}^{J\pi}(\text{comp.}) = \Big[\sum_{i \neq 1} \Theta_i^{J\pi} + \Theta_n^{J\pi}(\text{cont.}) \Big] \Big/ \Theta^{J\pi} \tag{83}$$

and the total inelastic cross section σ_{in} is the sum, Eq. (7), of compound and direct parts. The capture, fission, and (n,2n) cross sections σ_c, σ_f, and $\sigma_{n,2n}$ are given by Eq.(79) with

$$G_c^{J\pi} = \Theta_\gamma^{J\pi} \Big/ \Theta^{J\pi} \qquad G_f^{J\pi} = \Theta_f^{J\pi} \Big/ \Theta^{J\pi} \qquad G_{n,2n}^{J\pi} = \Theta_{n,2n}^{J\pi} \Big/ \Theta^{J\pi} \tag{84}$$

CONCLUSIONS

Pu-239 Calculations

Figure 4 shows σ_T and σ_{el} for Pu-239. The nuclear radius was chosen to fit σ_T at energies less than 2.5 MeV. When the same well parameters are applied to Cm-245,-247 it is reasonable to expect an error of 5%, especially at very small energies (E <0.1 MeV) where σ_T is sensitive to the choice of r_o. The good fit for σ_{el} below 2.5 MeV means that the optical model accurately computed σ_{se} and σ_a. Above 2.5 MeV, the compound elastic cross section is negligible and r_o was chosen to fit $\sigma_{el} \approx \sigma_{se}$. Attempts to fit both σ_T and σ_{el} for E ≥2.5 MeV had the effect of overestimating σ_a; this showed up clearly in the fission cross section. For this reason, only σ_{el} was fit above 2.5 MeV and σ_T and the direct inelastic cross section were adjusted as shown in Table 3.

The capture cross section shown in Figure 5 fits well at energies below 0.1 MeV but less well at higher energies. Since σ_c is small in the region of poor fit, the percent error is rather large (50%).

The fission cross section shown in Figure 6 was fit at four basic points. The height of the peak at 2 MeV is determined by E_{B_2}. The value of σ_f at 10 keV and the dip near 0.5 MeV are determined by E_B and E_c. The height of σ_f above the (n,nf) threshold is determined by a rough continuum model for Pu-238 fission. Since fission proceeds via compound nucleus formation, the ability to compute σ_f depends upon an adequate calculation of σ_a in the optical model.

The inelastic and (n,2n) cross sections are shown in Figure 7. The fit shows that the use of elastic penetrabilities for levels above the first two excited states is a workable approximation. It was found that the use of elastic penetrabilities for the first two excited states as well caused the inelastic cross section to be too large; therefore, the $T_{\ell j}(2^+)$ had to be used for these two states. The close fit for $\sigma_{n,2n}$ shows that the continuum neutron model works well in the CASCADE code.

In Figure 8 the direct inelastic cross sections for the first two excited states as computed by 2PLUS are compared with those found by Prince using JUPITER I. It is not surprising that the simpler code 2PLUS underestimates the direct inelastic cross sections by 25%.

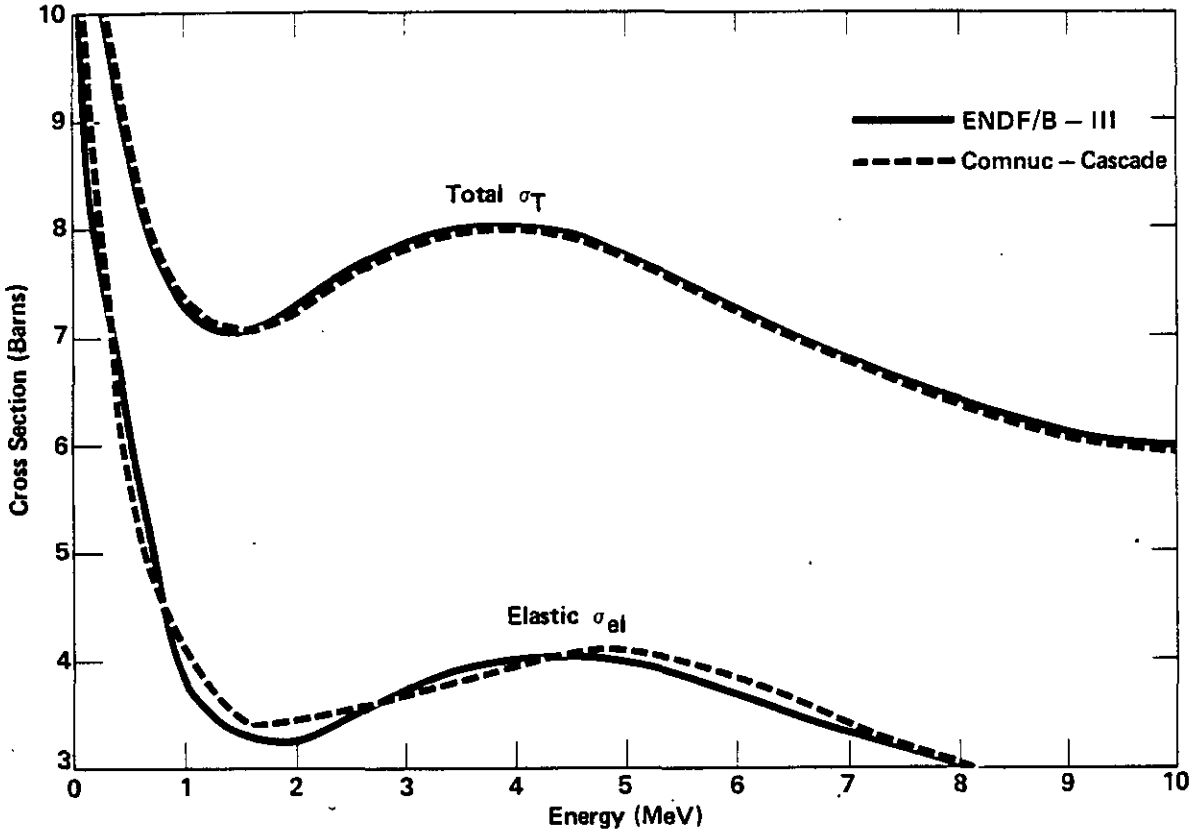

FIGURE 4. Total & Elastic Cross Sections (σ_T, σ_{el}) of Pu-239

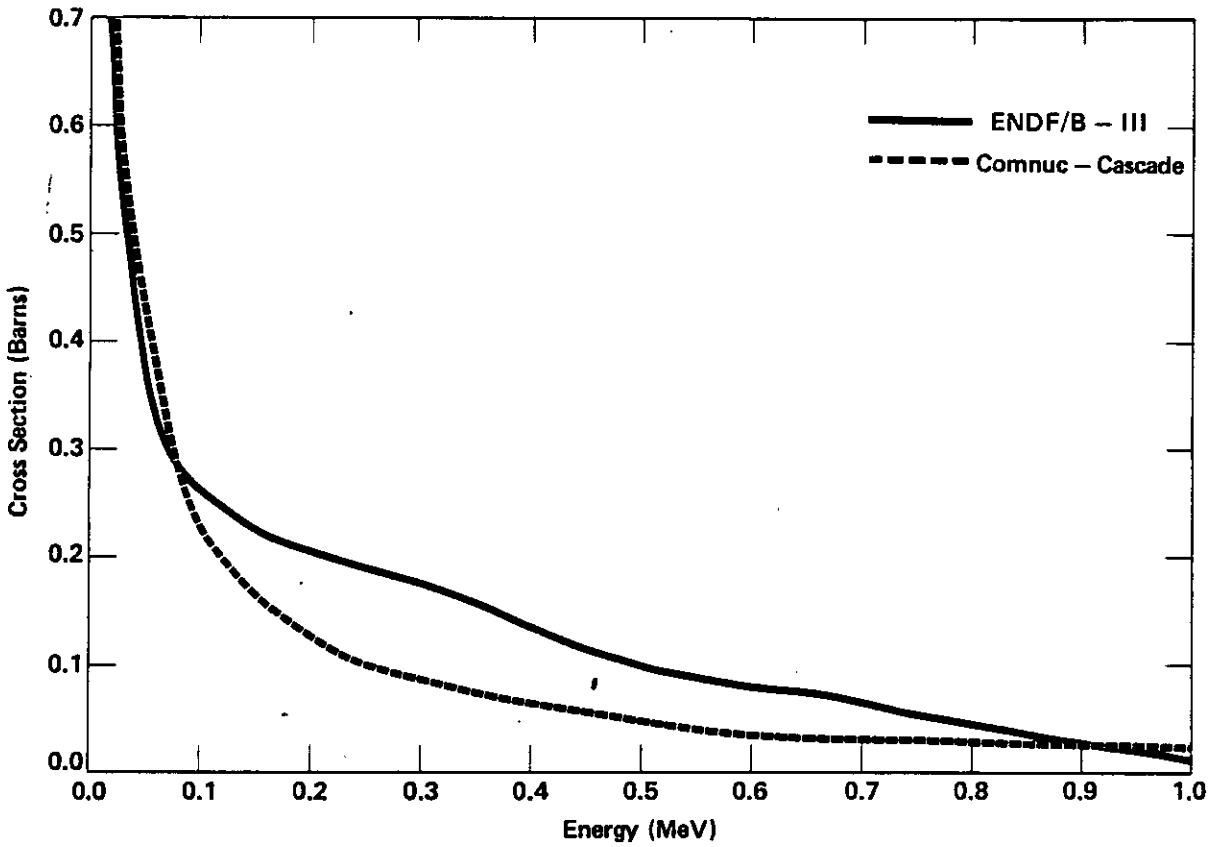

FIGURE 5. Radiative Capture Cross Section (σ_c) of Pu-239

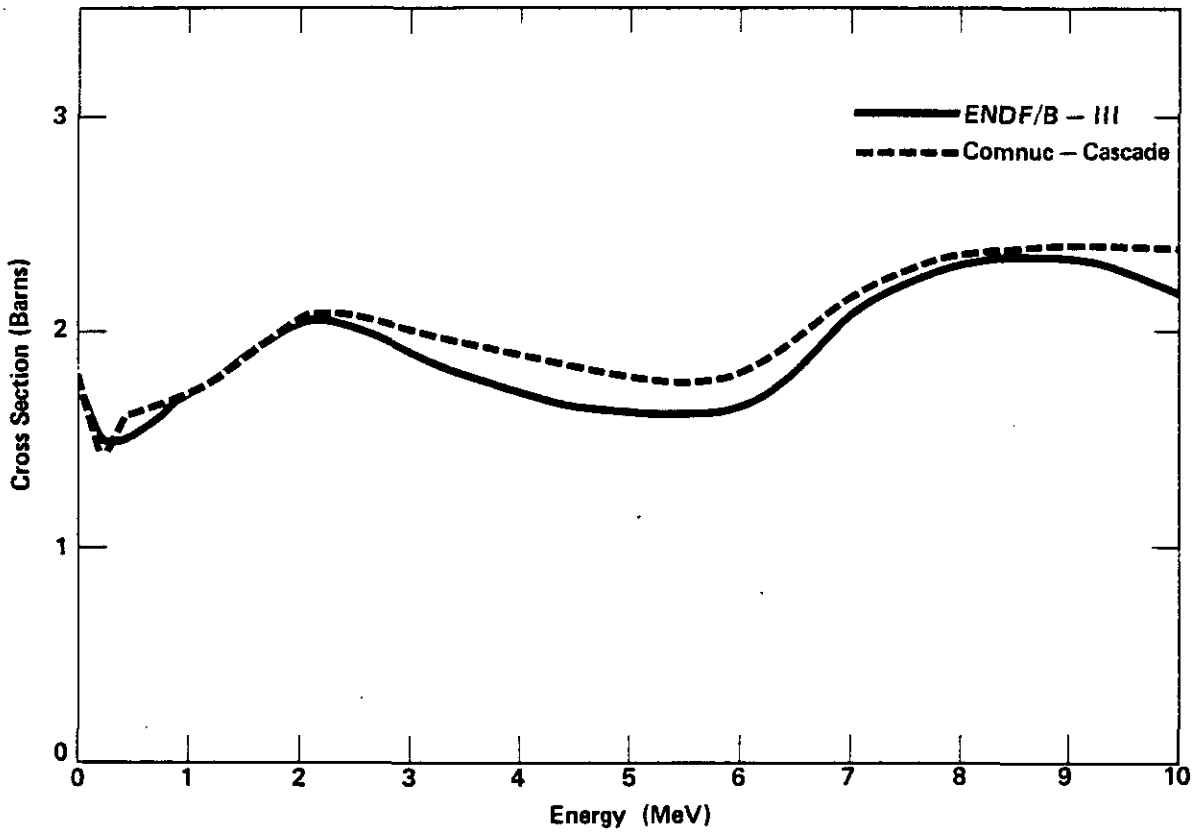

FIGURE 6. Fission Cross Section (σ_f) of Pu-239

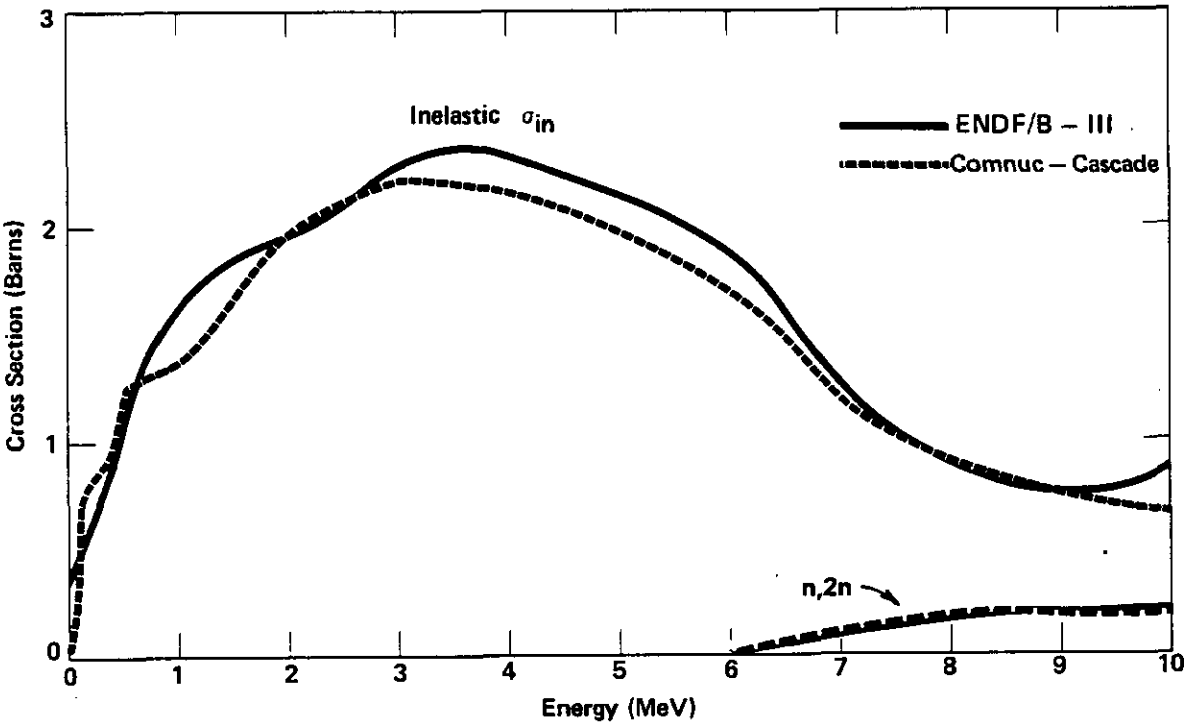

FIGURE 7. Inelastic and n,2n Cross Sections (σ_{in}, $\sigma_{n,2n}$) of Pu-239

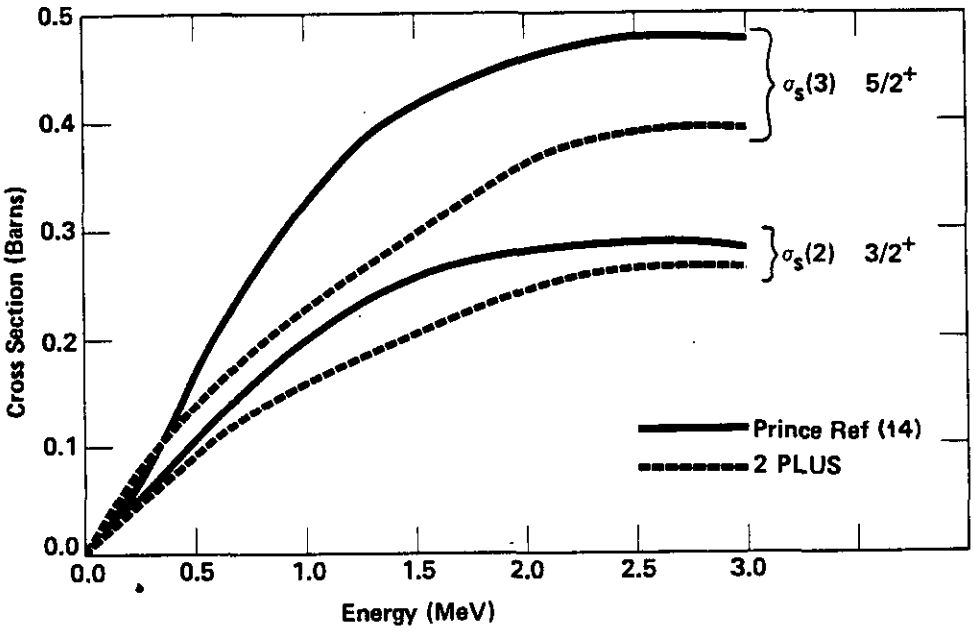

FIGURE 8. Direct Inelastic Cross Sections for First Two Excited States ($\sigma_s(2)$, $\sigma_s(3)$) of Pu-239

The Pu-239 calculations were undertaken only so that they could be used as a guide for the curium cross section calculations. It was found that the methods used for Pu-239 could be readily transferred to the curium isotopes.

Cm-245,-247 Calculations

The use of a large number of transition states in the discrete part of the fission model was necessary for the representation of σ_f at energies below 0.2 MeV. At these low energies the measured values of σ_f show fluctuations and the calculation gives only the trend of the cross sections.

The curium calculations would have been less useful without the fission data contained in Reference 32. Enough data were available so that the four basic fits that were used for the Pu-239 fission cross section could also be made for Cm-245,-247. Although the curium fission cross sections have not been measured above 3 MeV, the shape of the curve above this point is determined by the parameter E_{B_2} up to the (n,nf) threshold. Above the (n,nf) threshold rough continuum fission models for Cm-244,-246 are required, and these were also derivable from the data available in Reference 32. The fission cross sections for Cm-245,-247 are compared with measurements in Figures 9 and 10.

The fission cross section is a large part of the total cross section, and the accuracy of the other cross sections depends upon it. Given an adequate fission model, the accuracy of the elastic and inelastic cross sections depends primarily on the optical model calculations. These were seen to be quite good for Pu-239. The capture cross section is relatively small and errors in it would perturb σ_{el} and σ_{in} only slightly.

The high energy cross sections for Cm-245,-247 are given in Tables 8 and 9. The direct inelastic cross section is the total inelastic cross section (column 7) minus the compound inelastic cross section (column 6). The direct elastic and inelastic cross sections are shown explicitly in Tables 10 and 11. In these two tables and also in Tables 12 and 13 the compound elastic and inelastic cross sections are shown. Note that these become negligibly small above 3.0 MeV. For E >3.0 MeV, the inelastic cross section consists of the continuum contribution to the compound inelastic cross section plus the direct inelastic cross section. It is interesting to note that the direct inelastic cross section is a result of the nonspherical optical model, and this cross section makes a significant contribution to the total inelastic cross section at the higher energies.

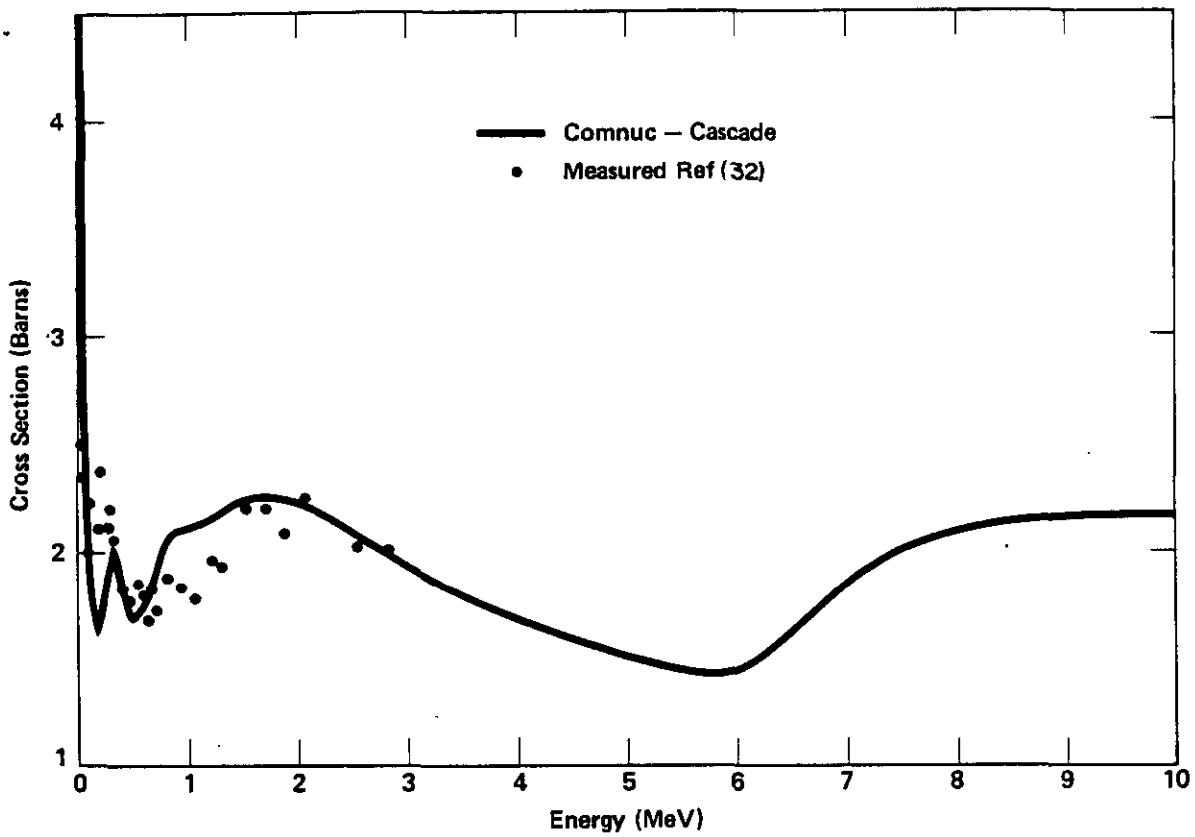

FIGURE 9. Fission Cross Section (σ_f) of Cm-245

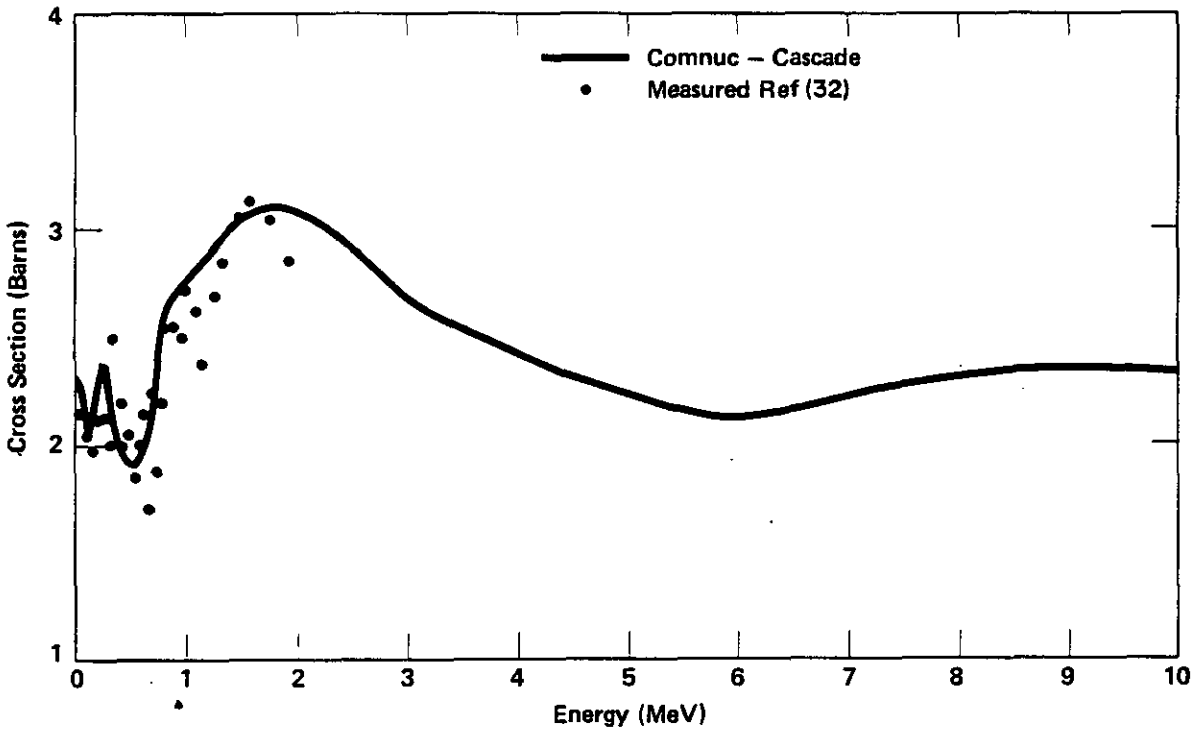

FIGURE 10. Fission Cross Section (σ_f) of Cm-247

TABLE 8

High Energy Neutron Cross Sections for Cm-245
(Cross Sections in Barns)

Energy, MeV	σ_T	σ_{el}	σ_c	σ_f	Comp. σ_{in}	Total σ_{in}	$\sigma_{n,2n}$
0.01	19.10	13.16	0.958	4.98			
0.03	16.94	13.17	0.550	3.22			
0.05	15.46	12.50	0.387	2.57			
0.06	15.03	12.22	0.327	2.38	0.098	0.104	
0.08	14.15	11.60	0.255	2.10	0.179	0.197	
0.1	13.26	10.68	0.223	1.92	0.370	0.438	
0.2	11.24	8.67	0.120	1.66	0.663	0.786	
0.3	10.29	6.98	0.074	2.02	1.04	1.22	
0.5	9.11	5.60	0.030	1.70	1.50	1.78	
0.8	8.04	4.59	0.018	2.09	0.970	1.34	
1.0	7.61	4.11	0.014	2.125	0.936	1.36	
1.2	7.41	3.77	0.011	2.16	1.00	1.47	
1.5	7.43	3.46	0.0086	2.24	1.16	1.72	
1.8	7.50	3.36	0.0064	2.25	1.27	1.88	
2.0	7.59	3.41	0.0051	2.23	1.305	1.94	
2.5	7.79	3.58	0.0026	2.08	1.305	2.13	
3.0	7.95	3.81	0.0012	1.91	1.25	2.23	
4.0	7.97	4.05	0.0002	1.69	1.19	2.23	
5.0	7.72	4.06	0.00005	1.49	1.225	2.17	
6.0	7.27	3.81	0.00002	1.45	1.14	1.96	0.049
7.0	6.80	3.43	0.00001	1.88	0.529	1.31	0.179
8.0	6.51	3.13		2.09	0.197	0.996	0.289
9.0	6.21	2.88		2.14	0.073	0.805	0.384
10.0	6.05	2.72		2.14	0.034	0.742	0.447

TABLE 9

High Energy Neutron Cross Sections for Cm-247
(Cross Sections in Barns)

Energy, MeV	σ_T	σ_{el}	σ_c	σ_f	Comp. σ_{in}	Total σ_{in}	$\sigma_{n,2n}$
0.01	21.18	17.64	1.23	2.31			
0.03	18.33	15.42	0.605	2.30			
0.05	16.52	13.84	0.420	2.255			
0.06	15.98	13.37	0.368	2.245			
0.08	14.95	12.38	0.288	2.15	0.117	0.135	
0.1	13.93	11.12	0.278	2.07	0.417	0.462	
0.2	11.55	8.23	0.152	2.38	0.656	0.788	
0.3	10.52	6.92	0.097	2.17	1.14	1.33	
0.5	9.32	5.70	0.050	1.92	1.35	1.65	
0.8	8.22	4.54	0.016	2.69	0.583	0.972	
1.0	7.76	4.06	0.0098	2.81	0.443	0.884	
1.2	7.57	3.74	0.0072	2.91	0.420	0.910	
1.5	7.58	3.47	0.0051	3.08	0.445	1.02	
1.8	7.62	3.40	0.0035	3.125	0.464	1.09	
2.0	7.67	3.46	0.0027	3.10	0.469	1.11	
2.5	7.84	3.64	0.0013	2.92	0.453	1.28	
3.0	7.96	3.86	0.0006	2.70	0.423	1.40	
4.0	7.96	4.07	0.0001	2.45	0.408	1.44	
5.0	7.72	4.08	0.00003	2.24	0.452	1.40	
6.0	7.28	3.84	0.00002	2.12	0.406	1.23	0.090
7.0	6.83	3.46	0.00001	2.22	0.205	0.991	0.156
8.0	6.52	3.16		2.30	0.083	0.883	0.178
9.0	6.23	2.91		2.34	0.034	0.768	0.207
10.0	6.04	2.74		2.34	0.019	0.730	0.230

TABLE 10

**Direct and Compound Elastic Cross Sections;
Direct and Compound Inelastic Cross Sections
for the First Excited State - Cm-245
(Cross Sections in Barns)**

Energy, MeV	$\sigma_s(1)$	$\sigma_r(1)$	$\sigma_s(2)$	$\sigma_r(2)$	$\sigma_{in}(2)$
0.01	7.23	5.93			
0.03	7.10	6.07			
0.05	6.78	5.72			
0.06	6.67	5.55	0.006	0.098	0.104
0.08	6.43	5.17	0.018	0.179	0.197
0.1	6.13	4.55	0.068	0.370	0.438
0.2	5.85	2.82	0.123	0.349	0.472
0.3	5.70	1.28	0.184	0.297	0.481
0.5	5.20	0.399	0.279	0.292	0.571
0.8	4.43	0.164	0.368	0.138	0.506
1.0	4.01	0.100	0.420	0.085	0.505
1.2	3.70	0.067	0.469	0.056	0.525
1.5	3.42	0.041	0.553	0.039	0.592
1.8	3.34	0.024	0.610	0.022	0.632
2.0	3.39	0.016	0.638	0.015	0.653
2.5	3.57	0.006	0.655	0.005	0.660
3.0	3.81	0.002	0.642	0.002	0.644

TABLE 11

Direct and Compound Elastic Cross Sections;
Direct and Compound Inelastic Cross Sections
for the First Excited State - Cm-247
(Cross Sections in Barns)

Energy, MeV	$\sigma_s(1)$	$\sigma_r(1)$	$\sigma_s(2)$	$\sigma_r(2)$	$\sigma_{in}(2)$
0.01	7.50	10.14			
0.03	7.65	7.77			
0.05	7.27	6.57			
0.06	7.14	6.23			
0.08	6.82	5.56	0.018	0.117	0.135
0.1	6.32	4.80	0.045	0.417	0.462
0.2	5.78	2.45	0.132	0.391	0.523
0.3	5.63	1.29	0.197	0.322	0.519
0.5	5.16	0.536	0.298	0.396	0.694
0.8	4.42	0.118	0.389	0.101	0.490
1.0	4.00	0.056	0.441	0.048	0.489
1.2	3.71	0.034	0.490	0.028	0.518
1.5	3.45	0.019	0.572	0.018	0.590
1.8	3.39	0.010	0.623	0.009	0.632
2.0	3.45	0.007	0.646	0.006	0.652
2.5	3.64	0.002	0.654	0.002	0.656
3.0	3.86	0.0006	0.636	0.0006	0.637

TABLE 12

Compound Inelastic Cross Sections for Levels Above the First Excited State - Cm-245
(Cross Sections in Barns)

Energy, MeV	$\sigma_p(3)$	$\sigma_r(4)$	$\sigma_r(5)$	$\sigma_r(6)$	$\sigma_r(7)$	$\sigma_r(8)$	$\sigma_r(9)$	$\sigma_r(10)$	$\sigma_r(11)$	$\sigma_r(12)$	$\sigma_r(13)$	$\sigma_r(14)$
0.2	0.314											
0.3	0.402	0.065	0.246	0.027								
0.5	0.183	0.063	0.206	0.249	0.075	0.169	0.148	0.069	0.049			
0.8	0.101	0.050	0.098	0.124	0.047	0.107	0.092	0.069	0.058	0.027	0.009	0.0045
1.0	0.070	0.0405	0.061	0.077	0.032	0.071	0.062	0.052	0.044	0.025	0.010	0.006
1.2	0.051	0.0325	0.042	0.052	0.023	0.050	0.044	0.039	0.034	0.021	0.010	0.006
1.5	0.034	0.024	0.026	0.032	0.016	0.031	0.028	0.026	0.023	0.016	0.009	0.005
1.8	0.021	0.016	0.017	0.020	0.0105	0.020	0.018	0.017	0.015	0.011	0.007	0.0035
2.0	0.015	0.011	0.012	0.014	0.008	0.014	0.013	0.012	0.011	0.008	0.005	0.003
2.5	0.005	0.004	0.004	0.005	0.003	0.005	0.005	0.005	0.004	0.0035	0.002	0.001
3.0	0.002	0.001	0.001	0.002	0.001	0.002	0.002	0.002	0.0015	0.001	0.0009	0.0005

TABLE 13

Compound Inelastic Cross Sections for Levels Above the First Excited State - Cm-247 (Cross Sections in Barns)

Energy, MeV	$\sigma_r(3)$	$\sigma_r(4)$	$\sigma_r(5)$	$\sigma_r(6)$	$\sigma_r(7)$	$\sigma_r(8)$	$\sigma_r(9)$	$\sigma_r(10)$
0.2	0.265							
0.3	0.400	0.179	0.235					
0.5	0.266	0.120	0.231	0.287	0.004	0.008	0.040	
0.8	0.078	0.033	0.058	0.074	0.003	0.009	0.023	0.040
1.0	0.041	0.018	0.030	0.037	0.002	0.006	0.014	0.022
1.2	0.026	0.012	0.019	0.023	0.002	0.005	0.009	0.015
1.5	0.016	0.008	0.011	0.013	0.001	0.003	0.006	0.009
1.8	0.009	0.005	0.007	0.008	0.001	0.002	0.004	0.005
2.0	0.006	0.003	0.005	0.005	0.0008	0.002	0.003	0.004
2.5	0.002	0.001	0.0015	0.002	0.0003	0.0007	0.001	0.0015
3.0	0.0006	0.0004	0.0005	0.0006	0.0001	0.0002	0.0004	0.0005

REFERENCES

1. R. W. Benjamin, F. J. McCrosson, V. D. Vandervelde, and T. C. Gorrell, DP-1394, E. I. du Pont de Nemours & Co., Savannah River Laboratory, Aiken, SC (1975).

2. M. K. Drake (Ed.), BNL-50274 (T-601), Vol. 1, Brookhaven National Laboratory, Upton, NY (1970).

3. R. W. Benjamin, F. J. McCrosson, and E. Gettys, DP-1447, E. I. du Pont de Nemours & Co., Savannah River Laboratory, Aiken, SC (1977).

4. C. L. Dunford, NAA-SR-11706, Atomics International (1966).

5. C. L. Dunford, TI-707-130-013, Atomics International (1971).

6. M. S. Moore and G. A. Keyworth, LA-DC-12230, Los Alamos National Laboratory, Los Alamos, NM (1970).

7. N. Bohr and J. A. Wheeler, Phys. Rev. 56, 424 (1939).

8. J. E. Lynn, UKAEA Report AERE-R7468, Harwell (1974).

9. H. Feshbach and V. F. Weisskopf, Phys. Rev. 76, 1550 (1949).

10. J. M. Blatt and V. F. Weisskopf, Theoretical Nuclear Physics, John Wiley (1952).

11. H. A. Bethe, Revs. Modern Phys. 9, 108 (1937).

12. H. Feshbach, C. E. Porter, and V. F. Weisskopf, Phys. Rev. 96, 448 (1954).

13. T. H. Braid, R. R. Chasman, J. R. Erskine, and A. M. Friedman, Phys. Rev. C4, 247 (1971).

14. A. Prince, Second International Conference on Nuclear Data for Reactors (Helsinki, 1970), II, page 825, IAEA, Vienna 1971.

15. R. R. Chasman, Phys. Rev. C1, 2144 (1970).

16. M. E. Rose, Elementary Theory of Angular Momentum, John Wiley (1957).

17. J. M. Blatt and L. C. Biedenharn, Revs. Modern Phys. 24, 258 (1952).

18. A. de-Shalit, Phys. Rev. 122, 1530 (1961).

19. J. L. C. Ford, Jr., Cheuk-Yin Wong, Taro Tamura, R. L. Robinson, and P. H. Stelson, Phys. Rev. 158, 1194 (1967).

20. S. G. Nilsson, Kgl. Danske Videnskab Selskab, Mat.-Fys. Medd. 29, No. 16 (1955).

21. P. F. Rose, J. M. Otter, E. Ottewitte, TI-707-130-026, Atomics International (1971).

22. C. M. Lederer, J. M. Hollander, and I. Perlman, Table of Isotopes, 6th Edition, John Wiley (1967).

23. C. L. Dunford, Atomics International Report AI-AEC-12931 (1970).

24. A. Gilbert and A. G. W. Cameron, Can. J. Phys. 43, 1446 (1965).

25. J. L. Cook, H. Ferguson, and A. R. de L. Musgrove, AAEC/TM392 (1967).

26. Kh. Maletski, L. B. Pikel'ner, I. M. Salamatin, and E. I. Sharapov, Second International Conference on Nuclear Data for Reactors (Helsinki, 1970). Translated by S. J. Amoretty, BNL-TR-350 (1970).

27. D. L. Hill and J. A. Wheeler, Phys. Rev. 89, 1102 (1952).

28. J. E. Lynn, The Theory of Neutron Resonance Reactions, Clarendon Press, Oxford (1968).

29. J. G. Cuninghame, K. Fritze, J. E. Lynn, and C. B. Webster, Nucl. Phys. 84, 49 (1966).

30. Y. Kikuchi and S. An, J. Nucl. Sci. & Tech. 5, 86 (1968).

31. A. Prince and M. K. Drake, Third Conference on Neutron Cross Sections and Technology, University of Tennessee, Knoxville, Vol. I, p. 418 (1971).

32. R. D. Baybarz, F. B. Simpson, M. E. Ennis, G. A. Keyworth, M. S. Moore, J. R. Berreth, W. K. Brown, R. R. Fullwood, J. H. McNally, and M. C. Thompson, LA-4566, Los Alamos National Laboratory, Los Alamos, NM (1970).